ICAS 2020 SHANGHAI
International Council of the Aeronautical Sciences
32nd Congress of the International Council of the Aeronautical Sciences
September 6-10, 2021
Pudong Shangri-La, Shanghai, China

EXPERIMENTAL STUDY OF THE DYNAMICS CHARACTERISTICS OF AN IMPACT WATER DROPLET ON SUPERHYDROPHOBIC SURFACE

Jingxin Wang[1], Chunling Zhu*[1.2], Zaili Yang[1], Chengxiang Zhu[1]

[1] Department of Aerospace Engineering, Nanjing University of Aeronautics and Astronautics, Nanjing, China.
[2] State Key Laboratory of Mechanics and Control of Mechanical Structures, Nanjing University of Aeronautics and Astronautics, Nanjing, Jiangsu,210016, China.

Abstract

Water droplet impacting on the surface structures is ubiquitous in nature, as well as has a great effect on the aircraft safety. The dynamics characteristics of a water droplet impacting on the superhydrophobic surface have been experimentally investigated and the impact behaviors are obtained by both the top and lateral view for capturing more details. The results show the impinging droplet undergoes rebound, receding breakup and splash by increasing impact velocity. Moreover, the droplet rebound can be prompted by increasing surface inclination, but inhibited by decreasing surface temperature. The supercooling surface has negative effect on the maximum spreading diameter, but the increase of surface subcooling has no obvious effect on the spreading regime. The fingering number and degree of rim deformation were enhanced by impact velocity but inhibited by surface inclination. Moreover, the rim disturbance showed a positive correlation with normal velocity but needed to consider inclination for large tilt.

Keywords: droplet, dynamic behaviors, superhydrophobic, rim disturbance

1. General Introduction

The droplets impacting on solid surfaces is a wide phenomenon encountered in nature, and is important to technical application, such as ink-jet printing [1], spray cooling [2], and aircraft icing [3]. The impacting and freezing of supercooled droplets on the wing will greatly severe aerodynamic effects, thus threat aircraft flight safety [4]. Various types of anti /de-icing methods are developed to overcome the problem. At present, superhydrophobic surface has been paid more attention as a passive anti-icing method, owing to the outstanding water repellency that could shorten contact time and decrease the wetting area [5]. Morphology of drop impinging on superhydrophobic surface exhibits more complicated flow pattern than the hydrophilic surface [6], including of spreading, fingering, deposition, receding, bouncing, sliding, and splashing, which attribute to the surface properties, e.g. roughness [7], wettability [6,8], inclination [9] and temperature [10, 11], and the properties of droplets, e.g. droplet size [12], impact velocity [13], density, viscosity [14], and surface tension [15]. Therefore, it is essential and meaningful to clearly understand the dynamics characteristics of droplet impacting on superhydrophobic surface for optimizing of anti-icing system.

Up to now, extensive investigations involving droplet impinging on superhydrophobic surface mainly focus on the maximum spreading factor, and splashing scenarios. Based on the total energy conservation relationship of surface energy, kinetic energy and viscous dissipation, the prediction equations of maximum spreading factor had been conducted [16, 17]. Besides, A few maximum spreading factor models were put forward on the account of the comprehensive contribution of capillary and viscous regimes [18, 19]. Splashing takes place at a relatively high drop impact velocities, and is accompanied by the production of tiny drops, which is crucial to aircraft icing. Rioboo et al. revealed three possible breakup and splash outcomes including of prompt splash, Corona

splash and receding break-up [20]. According to the experimental phenomena and empirical relations, the critical conditions for droplet splashing had been put forward [6, 21]. In addition, the droplet impacting behaviors on the inclined superhydrophobic surface have been investigated by some researchers. Antonini et al. found that the tilting could enhance drop rebound and reduce the rebound time [22]. Aboud et al. revealed that the maximum spreading diameter increased not only with Weber number, but also with the angle of incidence [23]. Ding et al. observed that the droplet rebounding process could be prompted by increasing surface inclination [24].

Recently, the dynamic behaviors of a water droplet impinging on the supercooled surface begins to attract research attention. In terms of horizontal surface, Roisman et al. found that the supercooled droplet rebound on cold superhydrophobic surface was significantly hindered, but the maximum spreading diameter was independent from surface temperature [25]. Shang et al. proved that the maximum spreading factor first descends and then increase with the increasing surface subcooling at a high Weber number, which attributed to the competition between the increased maximum fingering length and reduced maximum interior spreading diameter [10]. Unfortunately, the study of dynamics behaviors of droplet impinging on the cold superhydrophobic surface is still lacked, especially for the fingering pattern. That is, the complex effects of heat transfer and instability on the dynamic behaviors still far from complete understanding.

However, the most frequency-used method to measure the droplet shape was using high speed camera to record the impacting process from the side view. When the surface was inclined or uneven, the real droplet shape during the impact process would be much more complicated, and a 2-D profile cannot represent of the real shape [25]. Moreover, during the droplet spreading stage, especially for superhydrophobic surface with larger dynamic contact angle, the central region of the droplet was lower than the outer region, and thus the central region information was blocked by the outer rim. Hui Hu et al. achieved time-resolved measurements of the thickness distributions of the droplet/film during the entire impact process by digital image projection technique [26]. Unfortunately, for droplet impinging on superhydrophobic surface, the information of spreading diameter would be cover up. Yang et al. explored the behaviors of droplet impacting on the transparent superhydrophobic surface by simultaneously obtaining the images of both the top view and bottom view, and observed the generation of satellite droplets in spreading and retraction processes [27].

In the present research, the dynamic behaviors of a droplet impacting on superhydrophobic surface with various inclination and supercooling degrees were studied by coupling top view and lateral view. Thereby, the effect of superhydrophobic surface inclination and temperature were discussed on the maximum spreading factor, contact time and rim stability. The results could enrich understanding on the mechanism for the droplet dynamic behaviors on the supercooled and inclined superhydrophobic surface.

2. Experimental Methods

Figure 1 shows a schematic of the experimental system in the current research. Deionized water droplet was employed as the working fluid in lateral test and deionized water droplets mixed with 0.5% black ink was employed as the working fluid in top test for reducing transmission on the liquid surface. The properties of droplet mixed with black ink were same with deionized water droplet, but the residue would decrease repellency of superhydrophobic surface. A stainless capillary tube was used to generate droplets, which was adjusted to obtain the appropriate impact velocity. The droplet volume only depended on the outer diameter of the tube, which ensured droplet diameter was within 2.5 ± 0.03 mm. Flexible tube was applied to connect the stainless capillary tube and syringe pump (LSP01-2A, China). A superhydrophobic surface was used in the present experiment, which surface morphology was shown in Figure 1. Moreover, the superhydrophobic surface was placed on the upper surface of container, which was filled with cold liquid alcohol. Prior to the experiment of droplet impacting on the subcooling superhydrophobic surface, the desiccant was tiled at the chamber to reduce the humidity, then, the cooling chamber was cool down to decrease air temperature to -10

degrees. The process of the droplet impinging on the superhydrophobic surface was recorded using a high-speed camera (PCO.HS4) operated with a frame speed of 5000 fps from lateral and top view. For high Weber number, breakup and splash processes of the droplets could not be completely observed from lateral viewpoint. For these cases, view from top, facilitated detection satellite droplets generated from the rim of the spreading lamella. The diameter and impact velocity were measured in lateral view experiments, and remained almost unchanged in the top view experiments. This was because the height positions of stainless capillary tube and superhydrophobic surface remain the same. A good repeatability of the experiments was observed.

The shape of droplets become slightly elliptical before impact due to falling approach. In such case, the equivalent diameter of the droplet D_0 could be expressed as

$$\mathrm{D}_0 = (D_X D_Y^2)^{1/3} \tag{1}$$

Where D_x and D_y were measured horizontal and vertical droplet dimensions, respectively.

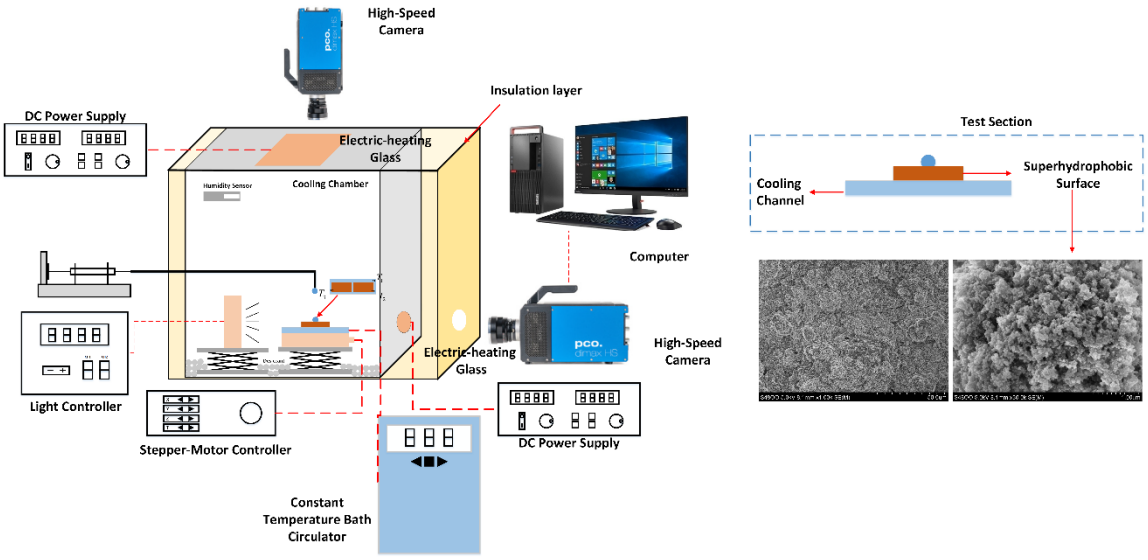

Figure 1 – Schematic of experimental system.

Table 1 –Value of relevant parameters.

Parameter	Value or Range
Density ρ	997.1kg·m-3
Surface tension σ	0.072N·m-1
Viscosity μ	0.898mPa·s
Impact velocity V_0	1.16-2.21m/s
Inclination of surface θ	0-60°
Surface temperature T_S	253.15-298.15K
Static contact angle	153° ±1°

3. Results and Discussion

3.1 Droplet impinging on superhydrophobic surface outcomes

The experiments of water droplet impacting on superhydrophobic surface with room temperature were carried out to understand the general behaviors of the droplet in the impacting process. The initial temperature of water droplet (T_w), air temperature (T_a), and surface temperature (T_s) were maintained at 298 K. The outcomes of droplet impacting on superhydrophobic surface are displayed from the lateral view, as shown in Figure 2. In general, the droplet impacting behaviors on the

superhydrophobic surface were consisted of three regimes: spreading, receding and rebounding. At initial stage, the top part of the droplet maintained spherical and bottom part contacted with the surface to form a lamella (t=1ms). Then, the droplet kept spreading until reaching the maximum diameter, which forms a pizza-like shape. However, for the case of large Weber number, the perturbation was generated at the rim. The perturbation could lead to the subsequent formation of satellite droplets, which would be defined as splash when occurred during spreading, but as receding break-up when occurred during retracting in this study.

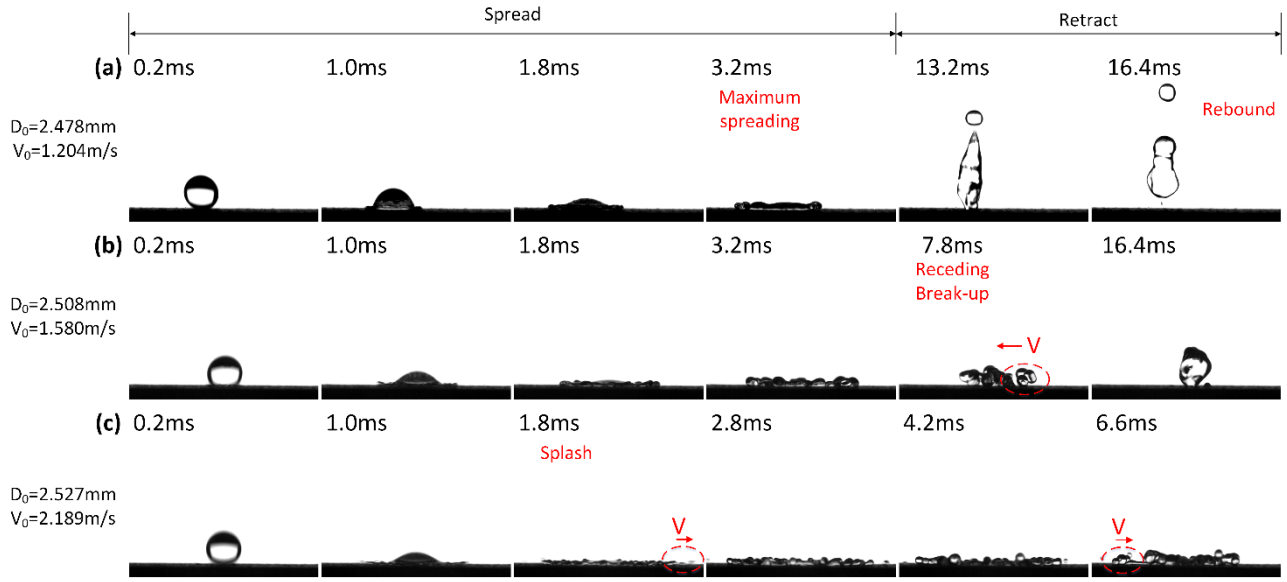

Figure 2 – Images of droplet impacting on the superhydrophobic surface with different velocities

To evaluate clearly the dynamic mechanism of droplet impinging, the top view experiments were carried out to show the impact process. However, for droplet impinging on superhydrophobic surface, the information of spreading diameter would be cover up due to large dynamic contact angle ($\theta_d > 90^{\circ}$), and the diameter and velocity of droplet could not be obtained directly in top view experiments. Thus, it was possible to prove the repeatability by comparing rim diameter from top view with ones from lateral view. For the top view experiment, the rim diameter could be get by distinguishing the droplet profile. The results of comparisons are shown in Figure 3. The result suggested that the trend of evolution process of rim diameter was similar, thus the coincidence was enough to evidence the repeatability of the experiments. In other words, the dynamic characteristics of droplet impinging could be explained by coupling with lateral view and top view. The reasons for the error bands were that, on the one hand, the superhydrophobic surface was uneven, which caused differences for inconsistent impact spots; on the other hand, the fingering pattern was variable along the circumferential direction, which was hard to display accurately by lateral view.

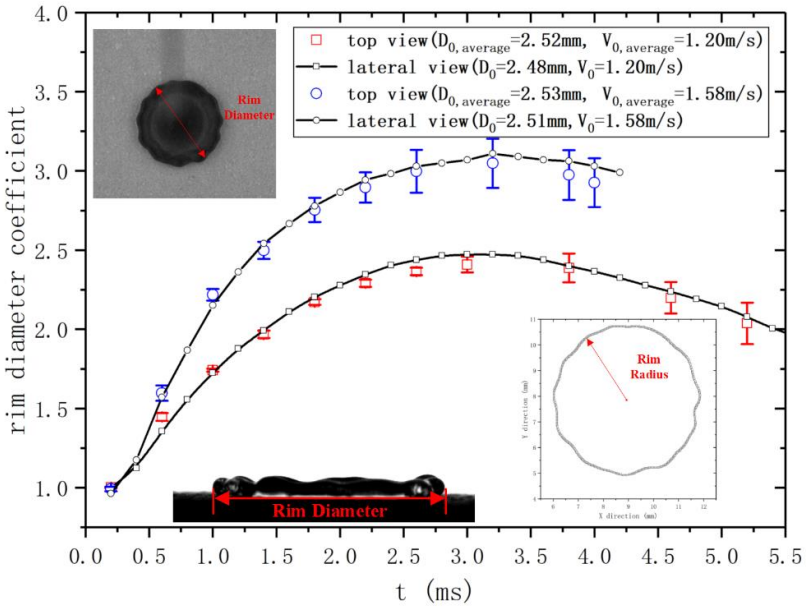

Figure 3 – Comparisons of rim diameter coefficient in different shoot directions

The lateral view had limitations on recording the process of droplet impact, thus the top view was provided to explain the mechanisms of different outcomes, as shown in Figure 4. It was clearly observed that the thin liquid lamella was eject from the bottom of droplet, and spreading rate increased with impact velocity. The liquid lamella could form the fingering pattern ascribed to Rayleigh-Taylor instability and intensified with the increase of impact velocity. Compared to the hydrophilic surface, more air was trapped between the droplet and superhydrophobic substrate. Besides, the rim thickness was higher than central liquid, thus the air pushed the liquid to the rim, which would strengthen the instability. Moreover, the liquid lamella could splash since large kinetic energy. The tiny water droplets were ejected radially from the rim during the spreading, and the remaining liquid began to retract. The perturbation of the rim or fingering pattern coalesced continuously during the receding, forming partial rebound finally. It was noted that the fingering pattern would be stretched, which led to breakup, or coalesced fingering pattern occurred to breakup due to the additional pressure on the bending position during the receding [27].

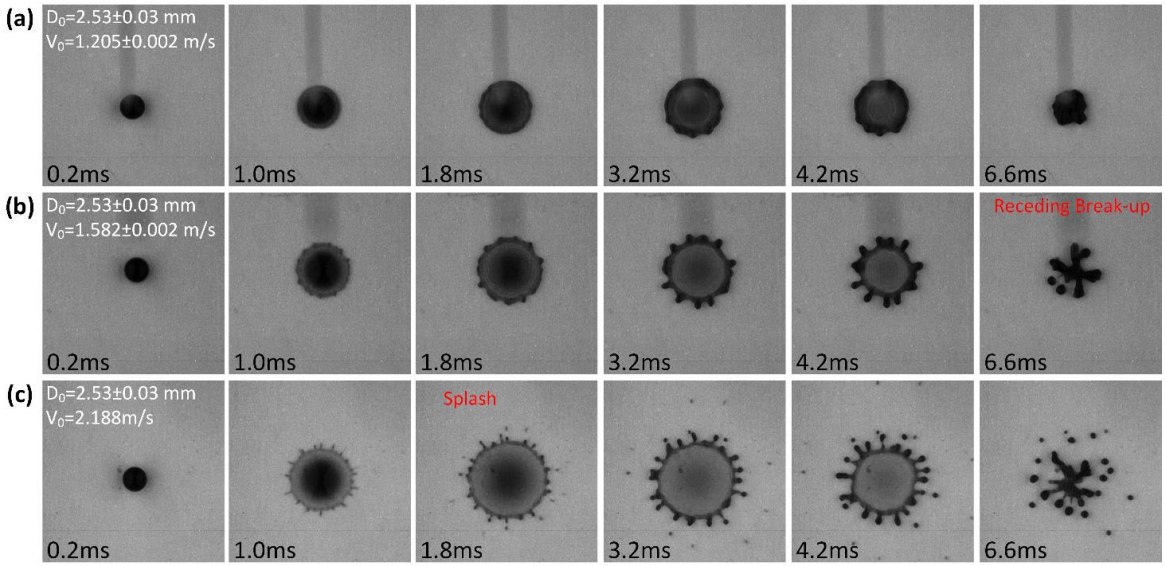

Figure 4 - Images of droplet impacting on the superhydrophobic surface from top view

3.2 Analysis of the impacting process

The maximum spreading diameter was an important parameter for droplet impinging on the solid surface, which had a great influence on the heat and mass transfer process. To better explain the spreading and retraction process of the droplet, a spreading factor (β) and dimensionless height (α) were introduced, which could be expressed as:

$$\beta = \frac{\mathrm{D}}{D_0} \tag{2}$$

$$\alpha = \frac{\mathrm{H}}{D_0} \tag{3}$$

Where D_0 is the initial equivalent diameter, D is the transient spreading diameter, H is the transient height of the primary droplet along the direction normal to the surface. In addition, the major dimensionless groups governing droplet impact include:

$$We = \frac{\rho V_0^2 D_0}{\sigma} \tag{4}$$

$$\mathrm{Re} = \frac{\rho V_0 D_0}{\mu} \tag{5}$$

$$t^* = \frac{t \times V_0}{D_0} \tag{6}$$

Figure 5 shows the evolution of β and α during the spreading and retraction process. It indicated that the maximum spreading factor β_{max} was larger at a higher impact velocity, attributed to the increased inertial force and kinetic energy. It was noted that the dimensionless time at maximum spreading t^*_{max} increased with impact velocity, however, the absolute time $t_{\max}$ remained the same. The result suggested that the impact velocity had little effect on the time at maximum spreading on the superhydrophobic surface. In addition, the α decreased firstly due to the falling of center liquid until the height of the rim was equal to the center liquid. The thickness of the rim was represent as the transient height of the droplet, thus the α rose slowly due to the increase of rim height. When the convex liquid column appeared in the center, α rose fast under the surface tension and extrusion of surrounding liquid. Thereafter, α rapidly decreased, attributed to the separation of secondary droplet.

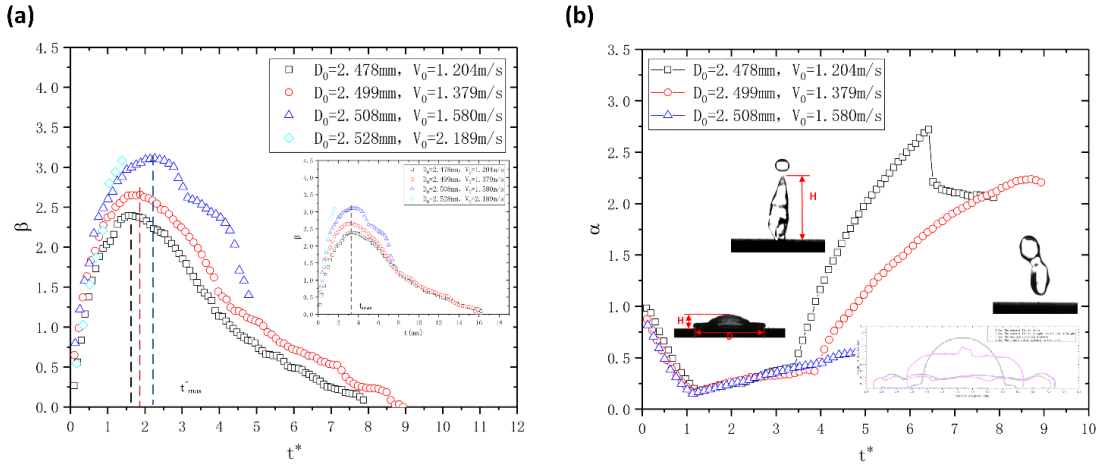

Figure 5 – Evolutions of droplet spreading factor and dimensionless height during the impinging process for various impact velocities

In practical applications, most of the device surface was inclined rather than horizontal. Thus, to explore the influence of surface inclination on the dynamic behaviors, a droplet impacting on the superhydrophobic surface with various inclination were studied. Compared with hydrophilic surface, droplet impacting on the tilt superhydrophobic was tend to rebound, and the sliding process was

obviously visible at small inclination. The instantaneous images in the impact process is shown in Figure 6.

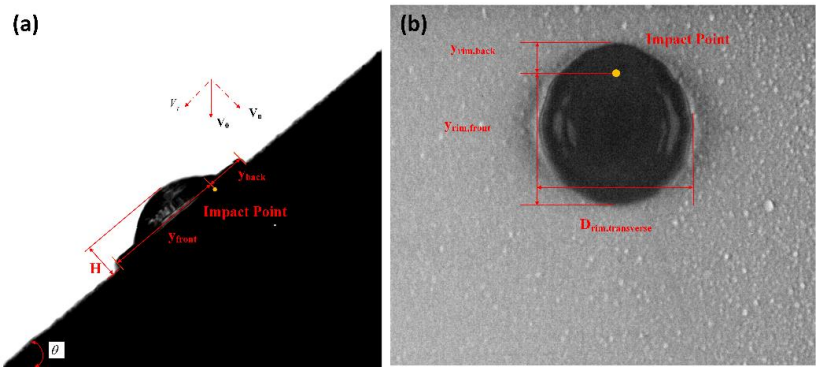

Figure 6 – Droplet impinging on the inclined superhydrophobic surface, (a) lateral view, (b) top view

The first phase of impact involved the initial deformation of the droplet was similar to the case of normal impact, but the sequence phase appeared to slide due to the inclination. The process of droplet impacting on tilt superhydrophobic surface are shown in Figure 7. It was clearly suggested that the droplet began to slide during the spreading, and the spreading diameter reached the maximum at 3ms. Then, the tail of droplet retracted with the help of surface tension, and front of droplet continued to spreading forward.

Figure 8 illustrates the effects of the inclination on the dynamic behaviors. The y_{back} firstly increased with time, and then decreased due to the retraction and slide. Here the changing role of inertia and gravitational forces could be recognized. In the initial phase, the inertia forces dominated, but gravity became more influential at later stages. It should be noted that the maximum spreading in the back direction was less for larger inclination, due to the small inertial forces associated with the low wall-normal velocity ($v_n = v_0 cos\theta$). Moreover, the droplet impinging barely spread in the back direction, as the inclination exceeded 60 degrees. Meanwhile, the y_{front} increased with the inclination, which was attributed to the larger wall-tangential velocity ($v_t = v_0 sin\theta$). In addition, although the slide was strengthened, the maximum spreading factor decreased with the increase of inclination, as shown in Figure 9. The height of droplet at the rebound was increased with the inclination. That meant, the droplet was tensile strengthen in the direction normal to the surface, which was contributed droplet to bounce off the surface. It was noted that the contact angle of droplet tail decreased, and became acute angle as the inclination achieved 40 degrees. It was because that the adhesion between the droplets and surface increased with an increase in the v_t [9].

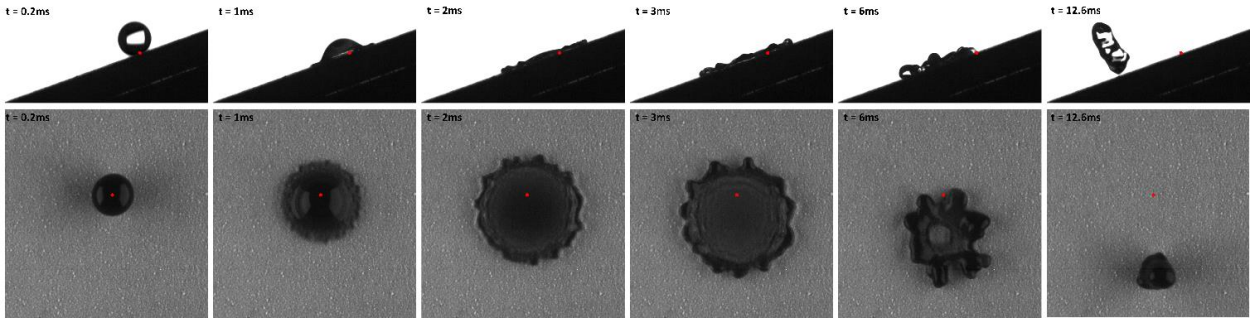

Figure 7 - Images of droplet impacting on the tilt superhydrophobic surface

$(\theta = 20^{\circ}, D_0 = 2.4mm, V_0 = 1.6m/s)$

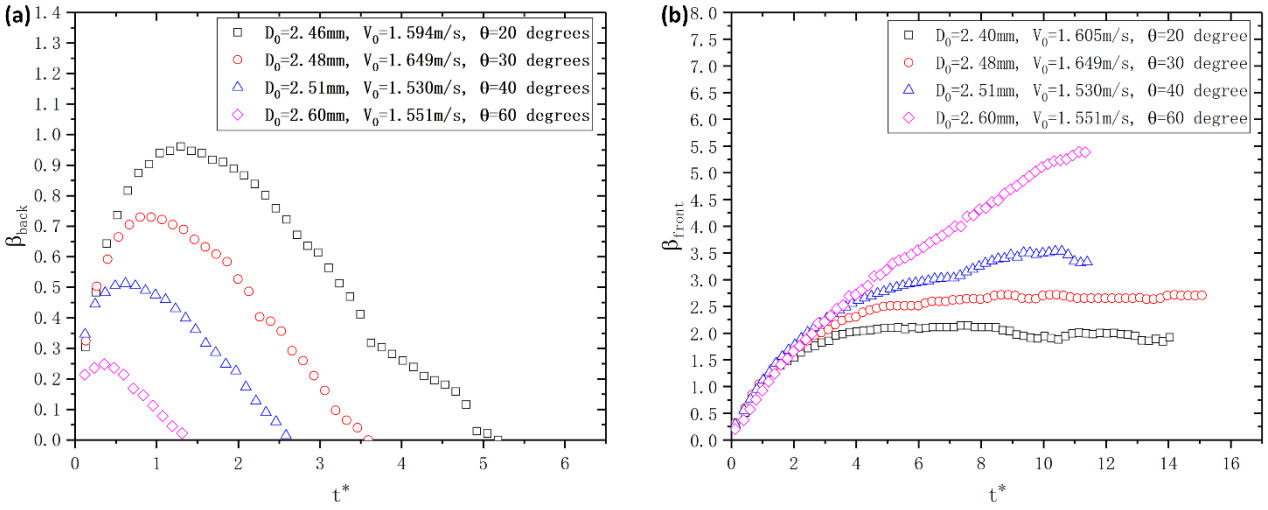

Figure 8 - Evolutions of droplet spreading factor for various inclination, (a) spreading factor of back direction, (b) spreading factor of front direction

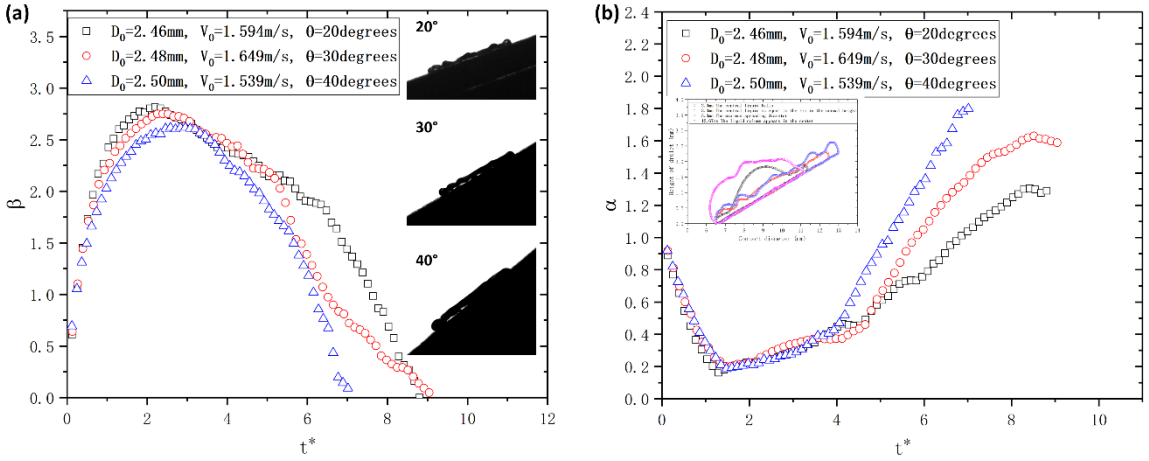

Figure 9 - Evolutions of droplet spreading factor and dimensionless height during the impinging regime for various inclination

In fact, the problems about the effect of surface temperature on droplet impact dynamics under a subcooling region are yet to be answered for the complex influences of droplet impact dynamics and heat transfer. Thus, the dynamic behaviors of a droplet impacting on the superhydrophobic surface with different supercooling degrees were studied. Prior to discuss the effect of supercooling degrees, as a basis of comparison, the experiment of a water droplet impacting on a superhydrophobic surface with room temperature was carried out. The result was consistent with the previous results, which the droplet appeared receding break-up and rebound. However, the droplet impinging on the subcooling superhydrophobic surface was inhibited from breaking. The evolutions of droplet impacting under different surface temperature were obtained and shown in Figure 10. The result suggested that the supercooling surface had negative effect on the maximum spreading diameter, but the degrees of supercooling had no obvious influences on the spreading regime of droplet. On one hand, the temperature of droplet impinging decreased during spreading due to the heat transfer from the droplet to the substrate, which led to an increase in the surface tension and viscosity. Thus, the maximum spreading diameter decreased due to the increased viscous dissipation and larger surface tension. On the other hand, the contact time of droplet impinging on the superhydrophobic surface was obviously shorter compared with the required time for droplets to reach subcooling from room

temperature. Thus, the analogous results for surfaces with various supercooling degrees were attributed to the insufficiency of the heat transfer between the droplet and superhydrophobic surface during the impact process. The dynamic characteristics of droplets impinging on the subcooling superhydrophobic surface could provide advantages for anti-icing system of aircraft.

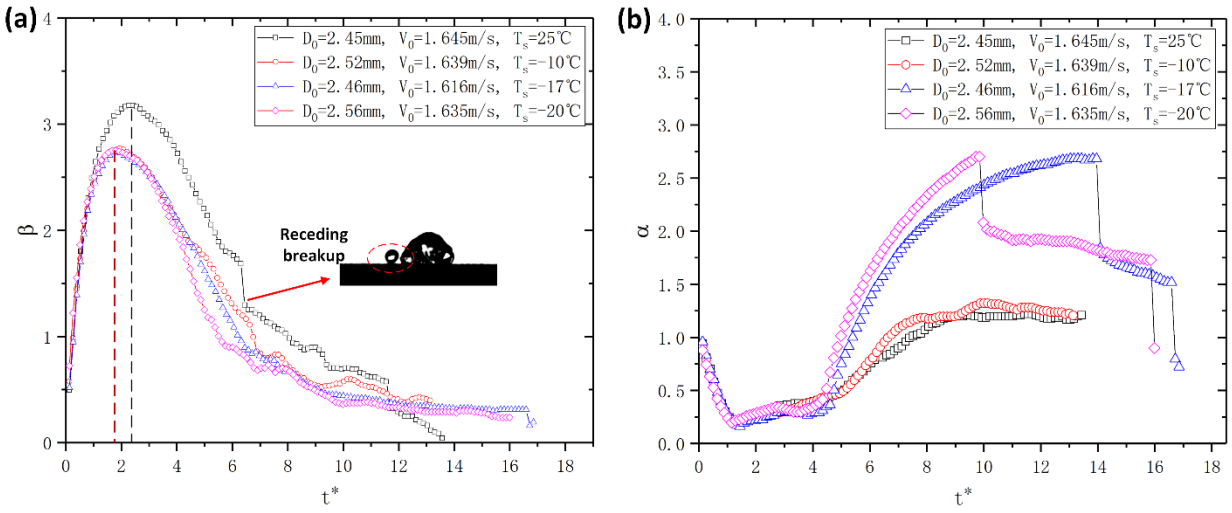

Figure 10 – Evolutions of droplet spreading factor and dimensionless height with various surface temperature

3.3 Rim disturbance

In the actual processes, the expanding rim of droplet impinging on the surface usually generate fingerlike perturbations around the edge of the spreading droplet, as shown in Figure 4. Unfortunately, no consensus has been reached about the underlying mechanism for the rim disturbance, which could lead to the fingering pattern formations and splashing. Compared with hydrophilic surface, the rim disturbance is easier to form for droplet impacting on the superhydrophobic surface. In order to characterize the degree of rim disturbance, the root-mean-square (RMS) was introduced, which could be expressed as:

$$\mathrm{RMS} = [\frac{1}{n}\sum_{i=1}^{n}(r_i - \bar{r})^2]^{1/2} \quad (7)$$

Where, n is the number of the collected values of the droplet rim, r_i is the radius at azimuth angle ϕ, $\bar{r}$ is the average radius of rim.

The snapshot sequences from the top view experiments made clear that, upon a surface, azimuthal undulations would appear over the rim of the spreading droplet. Before discussing the contributing factors of rim disturbance, the typical evolutionary process at the rim id worth noting. In order to observe the evolutions of rim disturbance intuitively, the rim profile of droplet impinging on the superhydrophobic surface was extracted, as shown in Figure 11. It was clearly indicated that the rim disturbance was intensified with time. At initial phase, the rim profile of droplet remained ideal ring, but the rim appeared undulations during the spreading. It was noted that the fingering pattern was stretched during the receding due to the coupling with tension force and viscous force.

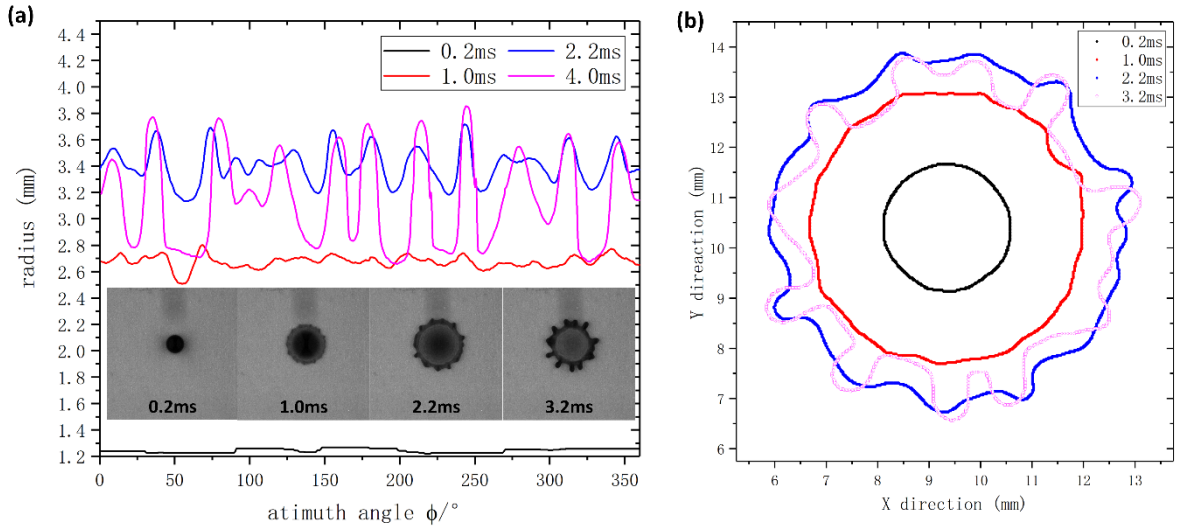

Figure 11 – Evolutions of droplet impacting on superhydrophobic surface, (a) Spatial signal droplet rim radius, (b) Rim profile of droplet

To reveal the effect of impact velocity, the rim disturbance at the moment of the maximum rim diameter is shown in Figure 12. The result suggested that the amplitude of the rim perturbations increased obviously with the impact velocity, and the valleys between spikes became narrower. That meant the number and length of fingering pattern increased with impact velocity. Moreover, the RMS increased with impact velocity. The distinctions on different impact velocity implied that the liquid-solid interaction beneath the droplet played a role in the evolution of frontal shape. When the impact velocity was large enough to generate a longer fingering pattern without splashing, the finger could break up and merge during retracting. Figure 13 shows the typical evolution of the fingering pattern during the retracting. Finger coalescence was one of the main causes of the decline in quantity of disturbance on the rim. The result suggested that two adjacent fingers get closer, and the trough between the two spines became narrower and shallower with receding, and finally, a coalescent finger was formed. Moreover, the neck between the fingers and the main droplet became thinner with receding, which added pressure on the bending position, and finally, a Satellite droplet was formed.

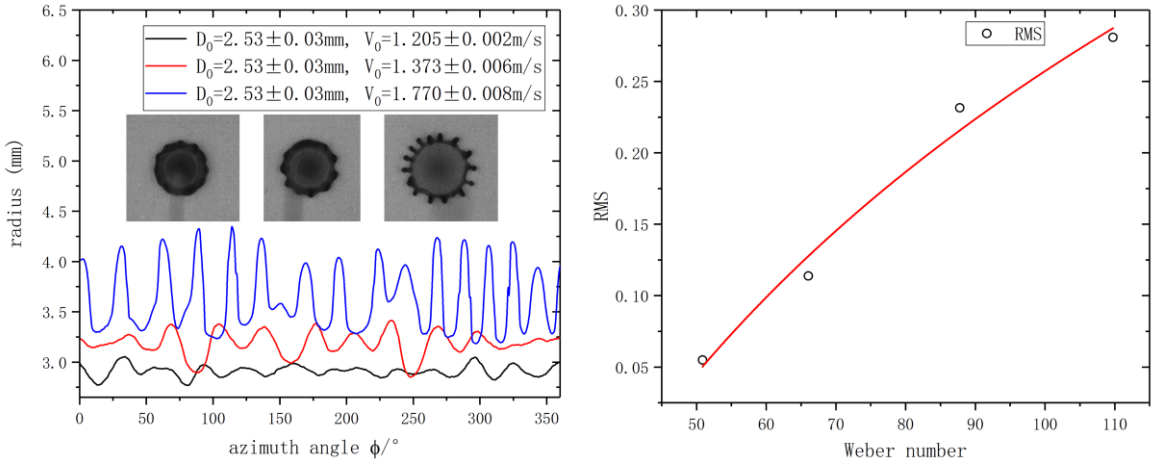

Figure 12 – Spatial signal sequence of droplet rim radius and RMS at various impact velocities

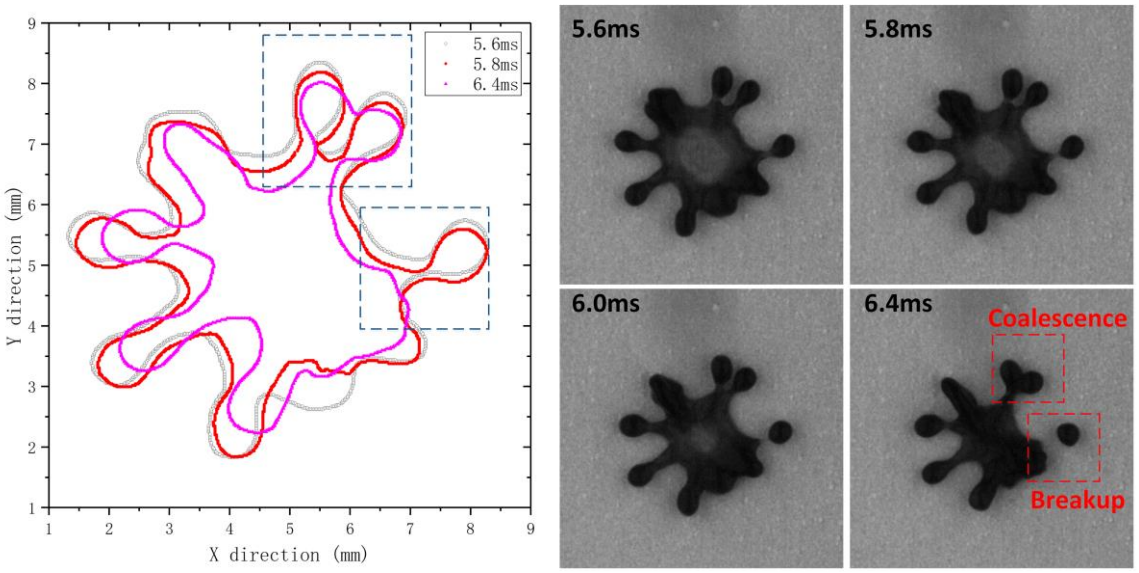

Figure 13 – The breakup and coalescence of a droplet impacting during the retracting

The tilt angle of the superhydrophobic surface has a great influence on the rim disturbance due to the coupling of impact velocity and gravity force. Figure 14 shows the rim disturbances of droplets impinging on the superhydrophobic surfaces with various inclination angles at the maximum transverse diameter. The result suggested that the amplitude and frequency decreased with the increase of the inclination, which indicated the rim disturbance gradually decreased. That was attributed to the lower wall-normal velocity. However, it was noted that the droplet tail appeared obvious protuberance as the inclination reached the 40 degrees. The protuberance aggravated with the increase of the tilt, and bounced off the superhydrophobic surface under the surface tension, as shown in Figure 15.

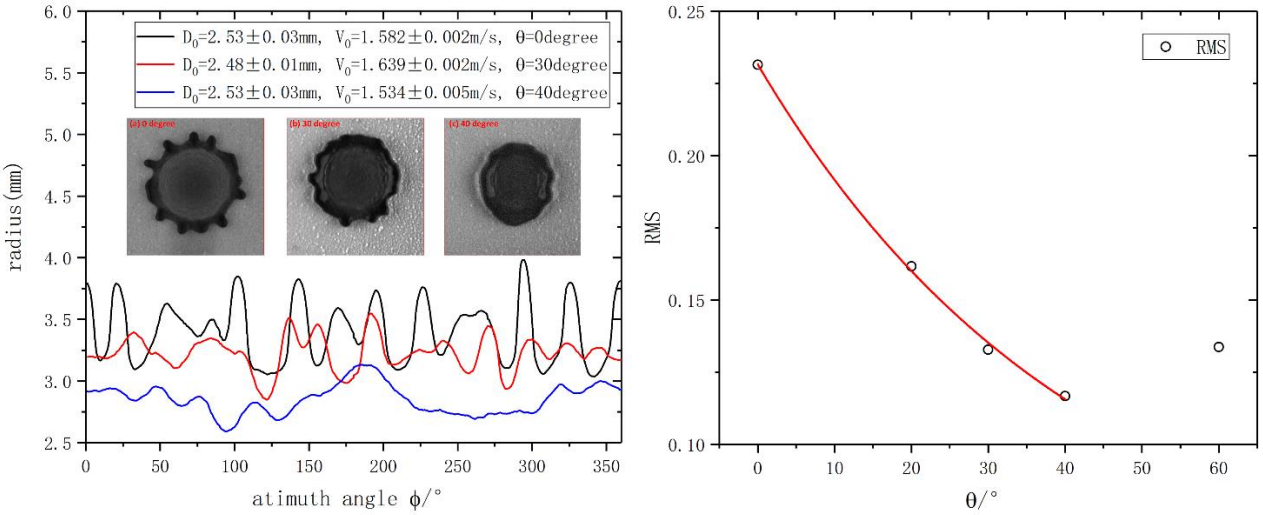

Figure 14 – Spatial signal sequence of droplet rim radius and RMS at various inclinations (3.2ms)

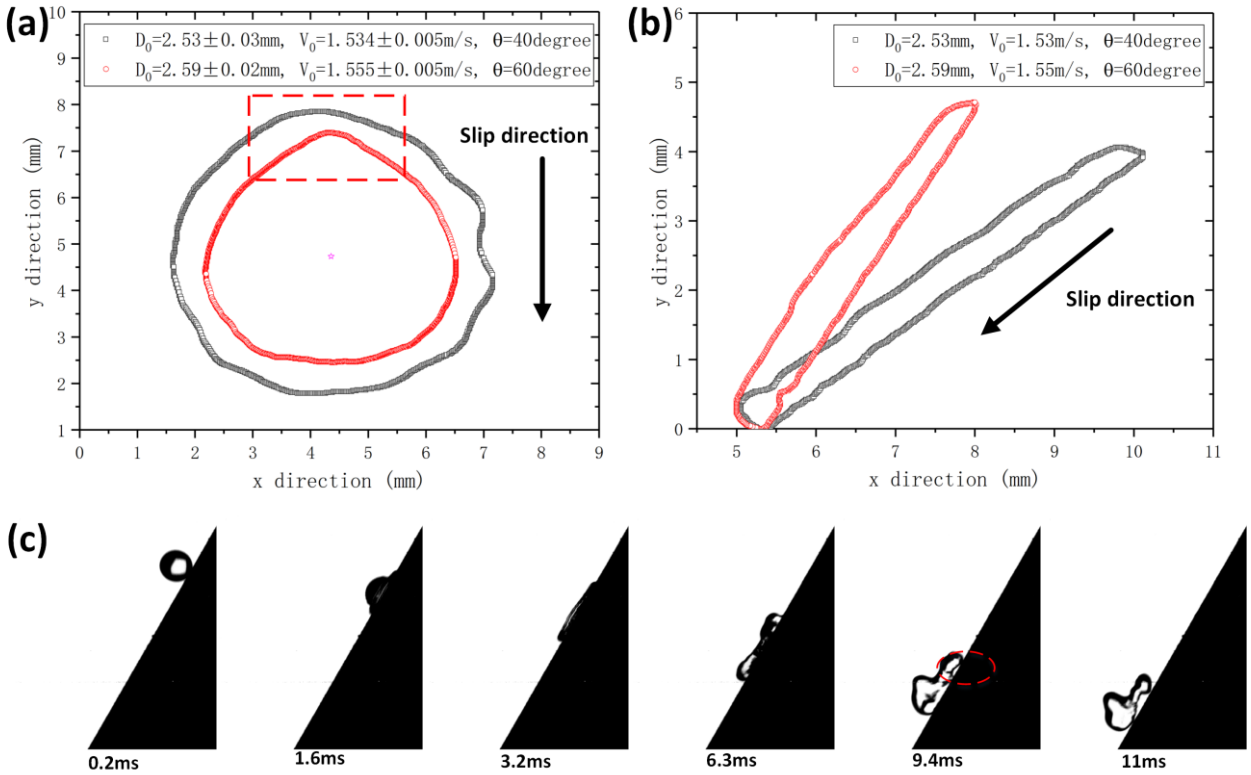

Figure 15 – droplet impinging on the superhydrophobic surface of 40 and 60 degrees inclination (a) Rim of droplet at 3.2ms; (b) profile of droplet at 3.2ms; (c)Images sequence of droplet impinging

3.4 The critical conditions of droplet impinging for different outcomes

In previous studies, there were two mechanisms for the prediction of the maximum spreading coefficient, including of energy conservation and momentum conservation. These typical correlations for the maximum spreading coefficient were listed in Table 2. In order to investigate the applicability of the models under different conditions, such as subcooling, the experimental results in this study were compared with the models in Figure 16. The result suggested that the predicated models overestimated the experimental ones in the low Weber number regime, but the model of Laan had a good agreement with experimental ones in the high Weber number regime. Unfortunately, the models above overestimated the experimental results of droplet impacting on the supercooling superhydrophobic surface regardless of the surface temperature. As a result, it is still difficult to obtain an accurate prediction for the maximum coefficient of a droplet impacting on a cold surface, thus it is the interest in the future.

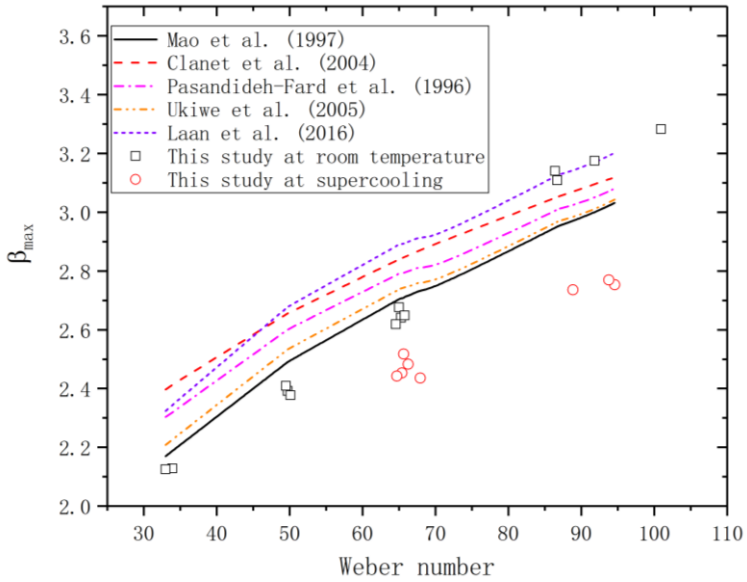

Figure 16 – Comparison between the experimental results in this study and the models

Table 2 Reported empirical models of the maximum spreading diameter factor

Reference	Equation
Mao et al. (1997) [16]	$[\frac{1}{4}(1-\cos\theta)+0.2\frac{We^{0.83}}{Re^{0.33}}](\beta_{max})^3-\left(\frac{We}{12}+1\right)\beta_{max}+\frac{2}{3}=0$
Clanet et al. (2004) [28]	$\beta_{max}=We^{\frac{1}{4}}$ for $(\frac{We}{Re^{1/5}}<1)$
Roisman (2009) [18]	$\beta_{max}\approx 0.87Re^{\frac{1}{5}}-0.4Re^{\frac{2}{5}}We^{-\frac{1}{2}}$
Pasandideh-Fard et al. (1996) [17]	$\beta_{max}=\sqrt{\frac{We+12}{3(1-cos\theta_a)+4(\frac{We}{\sqrt{Re}})}}$
Ukiwe et al. (2005) [29]	$(\mathrm{We}+12)\beta_{max}=8+\beta_{max}^3[3(1-cos\theta_Y)+4\frac{We}{\sqrt{Re}}]$
Laan et al. (2016) [19]	$\beta_{max}Re^{-\frac{1}{5}}=\frac{(WeRe^{-2/5})^{1/2}}{1.24+(WeRe^{-2/5})^{1/2}}$

Water droplet impacts on the superhydrophobic surface, showed different impact outcomes: rebound, receding breakup and splash (as shown in Figure 2 and Figure 4). Combined with the images sequences from top view, it could be easier to distinguish the outcomes. The drop impact outcome map is illustrated in Figure 17, where different outcomes were identified on the *We-Re* plane, for water droplet impacting on the superhydrophobic surface. The map showed that the droplet rebound occurred at $We < 70$. By increasing impact velocity or diameter of droplet, the droplet impinging were tend to break up during the retracting 70< We < 109. Moreover, the droplet impacting was tend to splash during spreading at large Weber region (*We* > 109) due to increase of rim disturbance. It was noted that the droplets impinging on the cold superhydrophobic were inhibited to occur receding breakup, and were tend to rebound partially.

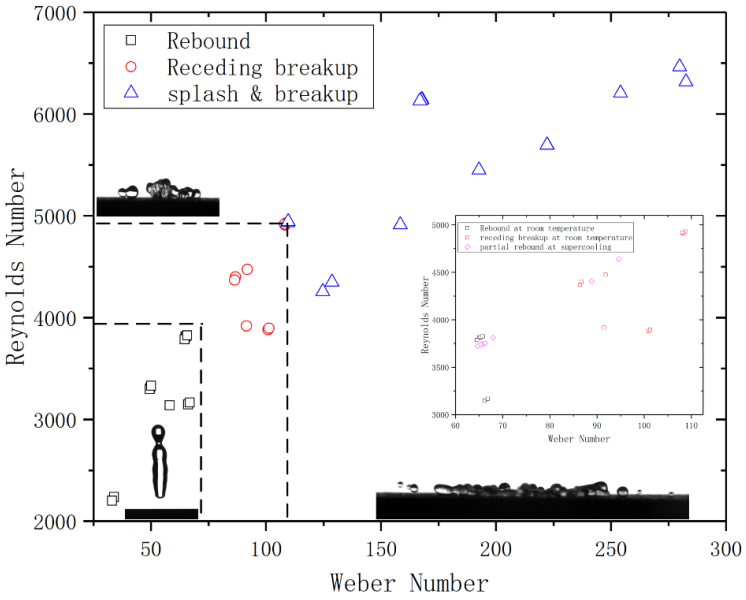

Figure 17 – Drop impact outcomes map for the superhydrophobic surface

4. Conclusion

The influences of impact velocity, surface inclination and temperature on the dynamic behaviors of a water droplet impinging on the superhydrophobic surface were experimentally explored. Moreover, the droplet impacting behaviors were observed from lateral and top view in terms of spreading factor, height factor, and evolutions of fingering pattern. According to the results and discussions, the following conclusions are derived:

- The maximum spreading diameter increased with the impact velocity. Moreover, the droplet underwent rebound, receding breakup and splash by increasing impact velocity.
- The droplet rebound could be prompted by increasing surface inclination, but inhibited by decreasing surface temperature. Moreover, the cold surface had negative effect on the maximum spreading diameter, but the increase of surface subcooling has no obvious effect on the spreading regime.
- The fingering number and degree of rim deformation were enhanced by impact velocity but inhibited by surface inclination. Moreover, the RMS was introduced to quantify the rim disturbance and showed a positive correlation with normal velocity but needed to consider inclination for large tilt.

5. Acknowledgments

The study is funded by the Natural Science Foundation of China (NSFC Grant No. 11832012), and the Research Fund of State Key Laboratory of Mechanics and Control of Mechanical Sturtures (Grant No. MCMS-I-0120G01).

6. Copyright Issues

7. Contact Author Email Address

Jingxin Wang: jxwang@nuaa.edu.cn ; Chunling Zhu: clzhu@nuaa.edu.cn ; Zaili Yang: 1182537992@qq.com ; Chengxiang Zhu: cxzhu@nuaa.edu.cn ;

8. Copyright Statement

References

[1] Van Dam D B and Le Clerc C. Experimental study of the impact of an ink-jet printed droplet on a solid substrate [J]. *Physics of Fluids*, Vol. 16, No. 9, pp 3403-3414, 2004.

[2] Roisman I V, Horvat K and Tropea C. Spray impact: rim transverse instability initiating fingering and splash, and description of a secondary spray [J]. *Physics of Fluids*, Vol. 18, No. 10, 102104, 2006.

[3] Norde E, Hospers J M, Van Der Weide E, et al. Aircraft icing in flight: effects of impact of supercooled large droplets [C]. *International Council of the Aeronautical Sciences (ICAS)*, St Petersburg Russia, 2014.

[4] Cao Y H, Tan W Y and Wu Z L. Aircraft icing: An ongoing threat to aviation safety [J]. *Aerospace Science and Technology*, Vol. 75, pp 353-385, 2018.

[5] Lin Y B, Chen H F, Wang G Y, et al. Recent Progress in Preparation and Anti-Icing Applications of Superhydrophobic Coatings [J]. *Coatings*, Vol. 8, No. 6, 208, 2018.

[6] Zhang H X, Zhang X W, Yi X, et al. Effect of wettability on droplet impact: spreading and splashing [J]. *Experimental Thermal and Fluid Science*, Vol. 124, No. 1, 110369, 2021.

[7] Shen J X and Wang X S. Substrate counts: Quantitative effects of surface roughness on fingering pattern and rim shape of an impacting drop [J]. *Physics of Fluids*, Vol. 32, No. 9, 093313, 2020.

[8] Liu C B, Liu Q and Lin Z H. Dynamical behavior of droplets transiently impacting on superhydrophobic microstructures [J]. *Physics of Fluids*, Vol. 32, No. 10, 103304, 2020.

[9] Ding B, Wang H, Zhu X, et al. Water droplet impact on superhydrophobic surfaces with various inclinations and supercooling degrees [J]. *International Journal of Heat and Mass Transfer*, Vol. 138, pp 844-851, 2019.

[10] Shang Y H, Zhang Y H, HOU Y, et al. Effects of surface subcooling on the spreading dynamics of an impact water droplet [J]. *Physics of Fluids*, Vol. 32, No. 12, 123309, 2020.

[11] Ding B, Wang H, Zhu X, et al. How supercooled superhydrophobic surfaces affect dynamic behaviors of impacting water droplets? [J]. *International Journal of Heat and Mass Transfer*, Vol. 124, pp 1025-1032, 2018.

[12] Gomaa H, Tembely M, Esmail N, et al. Impact of Micro-Droplets on Superhydrophobic and Hydrophilic Surfaces [C]. *Proceeding of the ASME 2014 4th Joint US-European Fluids Engineering Division Summer Meeting*, Chicago USA, Vol. 46216, V01AT05A008, 2014.

[13] Jung Y C and Bhushan B. Dynamic effects of bouncing water droplets on superhydrophobic surfaces [J]. *Langmuir*, Vol. 24, No. 12, pp 6262-6269, 2018.

[14] Kim J-H and Rothstein J P. Droplet impact dynamics on lubricant-infused superhydrophobic surfaces: The role of viscosity ratio [J]. *Langmuir*, Vol. 32, No. 40, pp 10166-10176, 2016.

[15] Baek S, Moon H S, Kim W, et al. Effect of liquid droplet surface tension on impact dynamics over hierarchical nanostructure surfaces [J]. *Nanoscale*, Vol. 10, No. 37, pp 17842-17851, 2018.

[16] Mao T, Kuhn D C, Tran H. Spread and rebound of liquid droplets upon impact on flat surfaces [J]. *AIChE Journal*, Vol. 43, No. 9, pp 2169-2179, 1997.

[17] Pasandideh-Fard M, Qiao Y, Chandra S, et al. Capillary effects during droplet impact on a solid surface [J]. *Physics of fluids*, Vol. 8, No. 3, pp 650-659, 1996.

[18] Roisman V I. Inertia dominated drop collisions. II. An analytical solution of the Navier–Stokes equations for a spreading viscous film [J]. *Physics of Fluids*, Vol. 21, No. 5, 296, 2009.

[19] Laan N, Bruin K D, Bartolo D, et al. Maximum Diameter of Impacting Liquid Droplets [J]. *Physical Review Applied*, Vol. 2, No. 4, 2014.

[20] Rioboo R, Tropea C and Marengo M. Outcomes from a drop impact on solid surfaces [J]. *Atomization and sprays*, Vol. 11, No. 2, 2001.

[21] Riboux G and Gordillo J M. Experiments of drops impacting a smooth solid surface: a model of the critical impact speed for drop splashing [J]. *Physical review letters*, Vol. 113, No. 2, 024507, 2014.

[22] Antonini C, Villa F and Marengo M. Oblique impacts of water drops onto hydrophobic and superhydrophobic surfaces: outcomes, timing, and rebound maps [J]. *Experiments in fluids*, Vol. 55, No. 4, pp 1-9, 2014.

[23] Aboud D and Kietzig A-M. On the oblique impact dynamics of drops on superhydrophobic surfaces. Part I: sliding length and maximum spreading diameter [J]. *Langmuir*, Vol. 34, No. 34, pp 9879-9888, 2018.

[24] Li H, Roisman V I and Tropea C. Influence of solidification on the impact of supercooled water drops onto cold surfaces [J]. *Experiments in Fluids*, Vol. 56, No. 6, pp 1-13, 2015.

[25]Josserand C, Thoroddsen S T. Drop impact on a solid surface [J]. Annual review of fluid mechanics, Vol. 48, pp 365-391, 2016.

[26]Li H X, Kai Z, Waldman R M, et al. Quantification of Dynamic Droplet Impact onto a Solid Surface by using a Digital Image Projection Technique [C]. *Proceedings of the 55th AIAA Aerospace Sciences Meeting*, Texas USA, 2017.

[27]Yang B H, Wang H, Zhu X, et al. Effect of velocity on behavior of droplet impacting superhydrophobic surface [J]. *Ciesc Journal*, Vol. 63, No. 10, pp 3027-3028, 2012.

[28]Clanet C, B éguin C, Richard D, et al. Maximal deformation of an impacting drop [J]. *Journal of Fluid Mechanics*, Vol. 517, 199, 2004.

[29]Ukiwe C, Kwok D Y. On the maximum spreading diameter of impacting droplets on well-prepared solid surfaces [J]. *Langmuir*, Vol. 21, No. 2, pp 666-673, 2005.